22

Assessment of Efficacy of "*b*" Value as a Seismic Precursor for Select Major Seismic Events

Deepali Gadkari[1] *and Soumyajit Mukherjee*[2,*]

[1] *Department of Geography, University of Mumbai, Kalina, Santacruz (E), Mumbai, Maharashtra, India*
[2] *Department of Earth Sciences, Indian Institute of Technology Bombay, Mumbai, Maharashtra, India*

**Author for Correspondence: soumyajitm@gmail.com*

Abstract

The "*b*" value is a seismic long-term precursor that indicates the state of crustal stress condition. The magnitude of "*b*" is the slope of the line of best fit when log (to the base 10) of earthquake frequency over a certain time period is plotted against the earthquake magnitude, following the Richter-Gutenberg equation. We demonstrate an inverse relationship between earthquake frequency and magnitude at specific locations. This means that the frequency of earthquakes with low magnitude can be more than that of higher-magnitude earthquakes. The decrease in the frequency of low-magnitude earthquakes, particularly in the seismically active areas, indicates stress accumulation. This is reflected in terms of lower "*b*" values before the major earthquakes. This article assesses the efficacy of temporal variations of *b*-values by applying it to a number of recent major earthquakes in Nepal, Sumatra, Japan, and Chile. The "*b*" values before the earthquakes drop significantly. It is also found that the "*b*" per se varies from region to region, but the temporal pattern of the value invariably shows lower trends before an impending earthquake. If a seismically active region is constantly monitored for the "*b*" value variations, it can reveal the stress regimes.

Keywords *Tectonics; Geodynamics; Deformation mechanism; Tectonic instability*

22.1 Introduction

> "... the problem of earthquake prediction remained one of the most important unsolved problems in geophysics ..."—Zalohar (2018)

Terrains that accumulate strain slowly can be vulnerable to seismicity (Landgraf et al. 2017). Earthquake prediction has always been a fascinating branch of seismology having rather limited success. The US National Academy of Sciences (1976) defines such prediction as

Handbook of Petroleum Geoscience: Exploration, Characterization, and Exploitation of Hydrocarbon Reservoirs, First Edition. Edited by Soumyajit Mukherjee, Swagato Dasgupta, Chandan Majumdar, Subhandip Mandal and Troyee Dasgupta.

the process that specifies the expected magnitude range, the geographical area within which it will occur, and the time interval within which it will happen, with sufficient accuracy so that the degree of success of the prediction can be gauged (Iyer 1976). The definition reveals that there are three important aspects of earthquake prediction, viz. location, magnitude, and time. Earthquake prediction, as a scientific discipline, started after the theory of plate tectonics, got well established around the 1960s. Japan, China, the USA, and the erstwhile USSR, undertook several earthquake prediction-related programs.

Seismicity falling within the omega-sequence is stated to be predictive in terms of timing and magnitude of seismicity. Also, the Cosserat model for Båth's law speculates periodic and geometric seismic sequences (Zalohar 2018). Earthquake prediction stands on three important milestones. (i) The concept of "seismic gap" (McCann et al. 1978). (ii) The observation that the ratio between P-velocity to S-velocity (V_p/V_s) drops ~15% and then recovers before medium and large earthquakes. (iii) Successful prediction of the Haicheng earthquake (4 February, 1975, $M = 7.3$).

Earthquake prediction depends on other factors such as availability and authenticity of seismic data/seismic records, velocities of seismic waves, electrical resistivity, and chemical composition of water in the source region, changes in atmospheric parameters, crustal deformations, etc. All these parameters can be used for earthquake prediction and therefore can be termed seismic precursors.

The present work uses the data published online by the National Earthquake Information Centre (NEIC) and United States Geological Survey (USGS). This data is not declustered (i.e. the foreshocks and aftershocks are not removed from the records). The "*b*" value depends on the frequency of earthquakes in a particular region over a unit time period. It is observed (Gutenberg and Richter 1944) that the frequency of earthquakes decreases significantly before a major earthquake occurs. The time period in which this decrease will take place varies from place to place. While analyzing the records for the "*b*" value, it is found that this period ranges widely from six months to five years. The frequency of earthquakes again starts increasing just before the main earthquake in the form of foreshocks. This period may vary from one year to a few hours. It is also noted that the magnitude of completeness (Woessner and Wiemer 2005) of the NEIC catalog is for $M > 4.0$. The catalog is not complete for $M < 4.0$. For some years, sufficient data has not been available and so "*b*" values could not be computed for those time periods (Japan Region: 1991–2000; Chilean Region: 1986–1992).

USGS catalog considers all earthquake magnitudes as *mb* (body wave magnitude), but the source magnitude is also mentioned for many earthquakes in the catalog (Mueller et al. 1997; Petersen et al. 2008).

The "*b*" values are computed by the least squares method. The slope of the line relating earthquake magnitude and the logarithm of the number of earthquakes (log frequency in the unit time period) of that magnitude is the "*b*" value for that particular time period.

$$\text{Log}\, N = a - b\,M \tag{22.1}$$

where *N*, number of earthquakes; *M*, magnitude (on Richter scale); constant *a*, intercept; *b*, slope of the line.

Rather than the actual value of *b*, the general trend of the *b*-value over the specified time period is important. This is because the actual values of "*b*" for a region depend on the

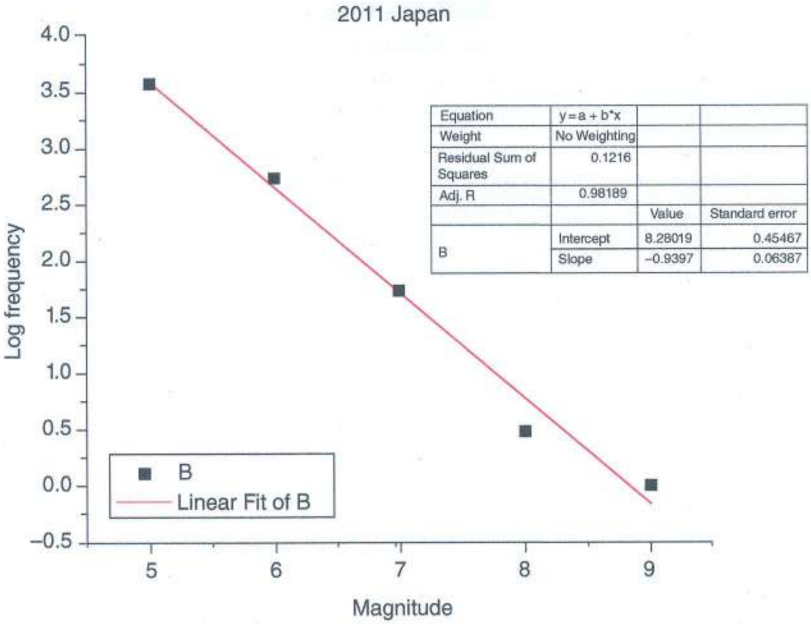

Figure 22.1 Computation of "*b*" values. Compare with Equation (2.1).

seismic characteristics of the areas. The frequency of earthquakes in each magnitude class (e.g. *M* 4.0–5.0) in each unit time period (one or five years) is the main input required to compute the "*b*" values (Figure 22.1). As this frequency differs from terrain to terrain, the "*b*" values of two different areas with different seismotectonics are not comparable. Computing a single "*b*" value for a region may not quantify how stress accumulates. The stress conditions vary with respect to the major impending earthquakes (Liu and Zhu 2010). Stress accumulates before major earthquakes over any region. This being a long-term process needs to be assessed over a considerable time span (>25 years). Therefore, the "*b*" values should be computed for consecutive unit time periods and then the trend be observed.

The "*b*" value remains to be one of the most important inferential statistical seismic precursors that indicate stress conditions in the area under consideration. Gutenberg and Richter (1944) demonstrated the relation between the earthquake frequency and its magnitude. Earthquakes though presumably momentary, are actually a process of slow accumulation and quick release of (crustal) stresses. An earthquake of a certain magnitude occurs when a region reaches the threshold beyond which crustal stress cannot be accumulated. A major earthquake demands a considerable accumulation of stress, which can imply an overall decrease in the frequency of earthquakes in the region. This can be reflected by lowering "*b*" values when observed over a particular time period.

The sensitivity of the *b*-value as a seismic precursor has been used by a number of researchers (e.g. Gibowicz 1973; Guha 1983; Patil et al. 1986; Utsu 1965). The 1967 Caracas earthquake occurred when the *b*-value crossed a maximum and when the standard deviation crossed a minimum (Fiedler 1974). Smith (1981) noted that before specific seismicity, the *b*-value elevates and then falls. Likewise, Huang and Turcotte (1988) referred seismicity to take place when the *b*-value crossed a threshold magnitude from several terrains. Post-earthquake studies confirmed a good correlation between a lowering trend in *b*-value and a major seismic event in the area. The examples include seven New Zealand earthquake sequences studied by Gibowicz (1973) in which *b*-values reduce initially before the main earthquake, increase after the main shock, and decrease again until the largest aftershock. He also noted during the earthquake swarm that the coefficient *b* decreases logarithmically with time. Profound lowering/variation (from 0.55 to 2.40) of *b*-value before seismicity, such as that reported from the Andaman-Sumatra region (Nuannin et al. 2005a, 2012), also remains valid for artificially induced seismicity (Nuannin et al. 2005b). Such lowering is conspicuous over a time scale of months or years, and a further time resolution is not possible (El Nader et al. 2016). Note that the *b*-value anomaly can also be caused by natural reasons other than seismicity, viz. significant heterogeneity of rocks, weak stress field, elevated thermal gradient, and reduced effective stress. The *b*-value can vary depth-wise as well in a single terrain (review in El Nader et al. 2016). Besides its temporal variation, a spatial disparity of *b*-values has been used to predict seismicity (Sobiesiak et al. 2007).

Ayyub and McCuen (2011) referred to a statistical cumulative transformation function to describe earthquake magnitudes (also see Zuniga and Wiemer 1999). A similar approach was found to be fruitful by Zuniga and Wyss (1995).

The present work assesses the efficacy of temporal variation of the *b*-value as a seismic precursor for four major seismic events from: (i) Nepal Himalaya; (ii) Sumatra region; (iii) Japan trench; and (iv) Chilean Coast (Figure 22.2).

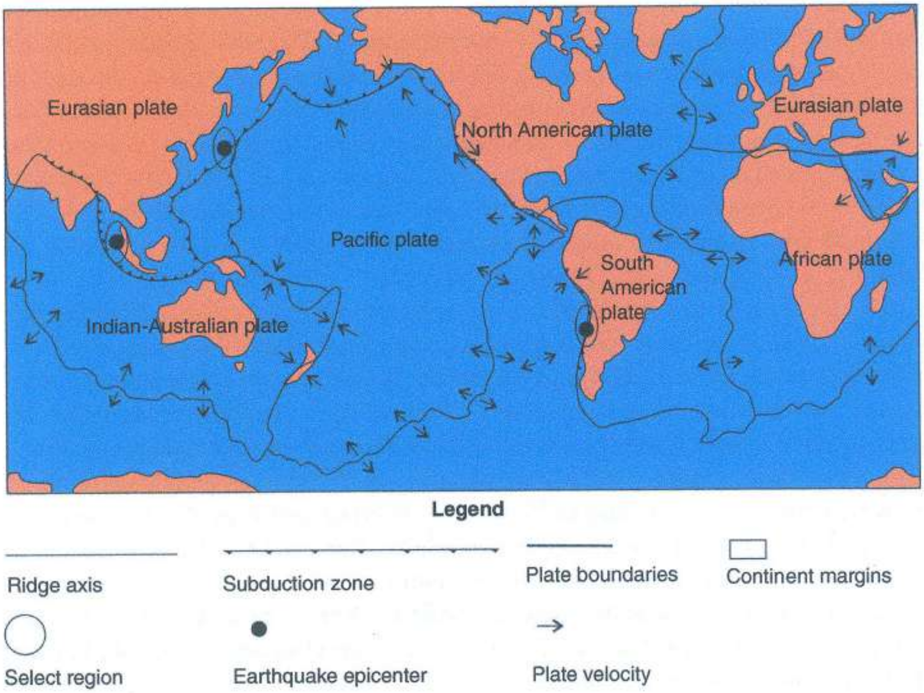

Figure 22.2 Locations of select earthquakes: (1) Nepal Himalayas, (2) Sumatra region, (3) Japan trench, and (4) Chilean Coast.

22.2 Tectonics of the Select Regions

22.2.1 Nepal Himalayas

Three major earthquakes in the Himalayas took place in the geological record: the 1905 Kangra (Mw 7.8), the 1934 Bihar-Nepal (Mw 8.2), and the 1950 Assam (Mw 8.6) earthquakes. Seismicity in the last ~100 years in the Himalayas has been well studied including in the Nepal region (review in Rajendran et al. 2017). The arc-parallel major faults, such as progressively northward the Main Frontal Thrust, the Main Boundary Thrust, and the Main Central Thrust are the active tectonic regions in the Himalayas. Whether an earthquake of magnitude >9 can strike the Himalayas has been recently debated geophysically (review in Wyss 2014). Out-of-sequence/active deformation zones pass through the Nepal Himalayas (review in Mukherjee 2015). Therefore, the Nepal Himalayas is considered seismogenic in general.

India-Eurasia collision-induced crustal shortening of the Greater-, Lesser-, and Siwalik regions of the far eastern Nepal Himalayas so far has been ~185–245 km (Schelling and Arita 1991). This estimate of shortening is, however, at least ~3 times less than what was proposed by DeCelles et al. (2001). The Siwalik equivalent Churia Zone is the most tectonically active part of the Nepalese Himalayas (Upreti 1999). However, seismicity in Nepal is also well-spread in the Lesser and the Greater Himalayas. Noting from a different viewpoint, seismicity in the Nepal Himalayas has been compiled in terms of its informally defined segments, viz. western, central, and eastern Himalayas. Singh et al. (2010) analyzed seismicity in the western Nepal Himalayas and noted that quiescence followed by seismicity is not ubiquitous in this region. They also predicted medium-sized earthquakes in this Himalayan segment from 2011 onward. Further, microseismicity has been documented from the Greater Himalayas, with ramp and flat geometry of major thrusts at the subsurface, since 1985 (Pandey et al. 1995). Pandey et al. (1999) pointed out that both the far eastern and the far western parts of the Nepal Himalayas are more seismic. Bollinger et al. (2007) reported that the small- and moderate-sized earthquakes in Nepal, in general, during 1995–2000 took place more in winter than during the summer. They postulated that the water contributed by the rainy seasons before the winter seasons augmented the Coulomb failure.

22.2.2 Sumatra Region

A rather up-to-date review of tectonics of the Sundaland is available in Metcalfe (2011). A sinistral slip separated the Australian and the Bird's Head along with the convergence in the New Guinea fold-and-thrust belt (McCaffrey 1989). The Bird's Head lithosphere is subducted below the Seram trough at ~300 km depth. Overall the Bird's head has been moving westward (Das 2004). Tectonic inversion in Sumatra that started in Late Miocene and has been continuing today is linked with a strike-slip deformation (Daly et al. 1991). The Sumatran Fault is a megascopic dextral strike-slip fault. Prawirodirdjo et al. (2000) deduced a 20-km depth of this fault at a specific location. Lasitha et al. (2006) reported that from 1900 to 2000, the slip rate for the Sumatra-Java arc varied unusually from 1 to 29 mm $year^{-1}$, and that the slip rate of the Sumatran Fault Zone has been 30–50 mm $year^{-1}$.

Regions nearby to this fault have recently been affected by the aftershocks of the 2004 Sumatra-Andaman quake (Mw 9; Engdahl et al. 2007). Sukmono et al. (1997) established a link between earthquake recurrence related to the Sumatran Fault and a fault segment geometric parameter. The relationship between the Sumatran Fault and the subduction zone has been debated (Lange et al. 2010) and still requires more study to comment on the relation between this fault and the nearby seismicity (McCaffrey 2009).

22.2.3 Japan Trench

The Japanese island represents an active subduction-related orogenic front (Isozaki et al. 2010). These islands were formed by the accretion of Permian, Jurassic, and Cretaceous rocks. As the Japan Sea opened 20–15 Ma ago, the islands attained the present position (review in Shikazono 2012). The Japan trench margin has been described as a …*homogeneous wedge of deformable, noncohesive Coulomb material during seamount subduction* (Lallemand and Le Pichon 1987). The Pacific Plate has been subducting below the Japanese islands along the Japan Trench with variable intraplate coupling and producing mainly thrust-type earthquakes (Miura et al. 2003 and references therein; also see Mogi 1990). Seismicity (>M 7.5) commonly displays an uneven epicenter distribution along this structurally varying trench with an intraplate sedimentary unit governing the release of shear stress (Tsuru et al. 2002). Specifically, the Nankai trough has been a place of vigorous seismicity with a recurrence interval of 100–200 years (Kodaira et al. 2002). The Philippine Sea Slab subducts with 10–40° dip along the Nankai trough (Xu and Kono 2002). Subduction followed by erosion of the seamounts along the Nankai trough might hinder segmentation of the seismogenic rupturing (Bangs et al. 2006), or even acted as a barrier to earthquakes (Kodaira et al. 2002). The mode of earthquakes varies along the Japan trench due to the differing roughness of the subducting plate (Tanioka 1997).

22.2.4 Chilean Region

The Chilean coast usually shows along-strike variation in tectonics (Gerbault et al. 2009, and its references). The maximum principal compressive stress axis (σ_1) in central Chile trends NW and E (Barrientos et al. 2004). Seismicity studies so far, however, indicated that the Chilean coast is basically a two-layered Benioff zone (Malgrange et al. 1981). Tassara and Echaurren (2012) referred to ~ 66 mm year^{-1} of convergence rate at the Andean Subduction Zone, which is the longest subduction zone in the world.

Stauder (1973) categorized and analyzed seismicity in the Chilean region but that did not include the *b*-values. The southern Chilean region has been divided into several seismic areas, but here again, the *b*-values have not yet been analyzed (Perucca and Bastias 2008). Along with other subsurface geophysical details, note the intermediate-depth seismicity does not belong to the Andean Subduction Zone (The ANCORP Working Group 1999). Principal stress axes orientation has been deduced from 20 to 50 km-deep locked zone in the northern Chile portion of the Andean Subduction Zone. Interestingly, this depth range is the zone where the hypocenters occur (Delouis et al. 1996). Lange et al. (2007) linked the spatial distribution of seismicity in the southern portion of the Chilean region fundamentally with the age and temperature of the oceanic plate.

The Chilean coast parallels the Andes Mountains chain. This chain varies in dip, age, and obliquity of the subducting slab. The Andean Subduction zone and the Chilean margin are characterized by a ramp and flat structure at depth (Farias et al. 2010). NW-striking steeply dipping reverse faulting has been deciphered based on fault plane solutions from the Andes Mountains (Suarez et al. 1983). Gerbault et al.'s (2009) numerical modeling demonstrated that the strength of the continental crust and that of the subduction channel governs the crustal shortening in this mountain chain (Gerbault et al. 2009).

Deformation in the central and southern Andes (22 °S–42 °S) is characterized by a seismicity cycle and an interseismic phase (Klotz et al. 2001). A nearly aseismic region exists in the Andes between 36 °S and 40 °S latitudes in between the ~NW trending Bio-Bio and the Gastre Fault zones – a zone of very high uplift by antiformal stacking (Bohm et al. 2002 and its references).

22.2.5 Data and Methods

Computation of "*b*" values requires considering two parameters of seismicity: (i) time interval, and (ii) magnitude interval/classes. The trend of "*b*" values over a time span is assessed with respect to the major seismic events in the region. Therefore, the optimum time interval for *b*-values computation is to be selected. This interval would depend on the seismotectonics of the areas. If frequently recurred and well documented, the time interval should be taken as <1 year. But in case of unavailability of seismic records, particularly those of the lower magnitudes, the interval can range 2–5 years.

A large number of earthquake records are required to link *b*-values with seismicity. Figure 22.3 represents the methodology followed for the "*b*" value computation and how

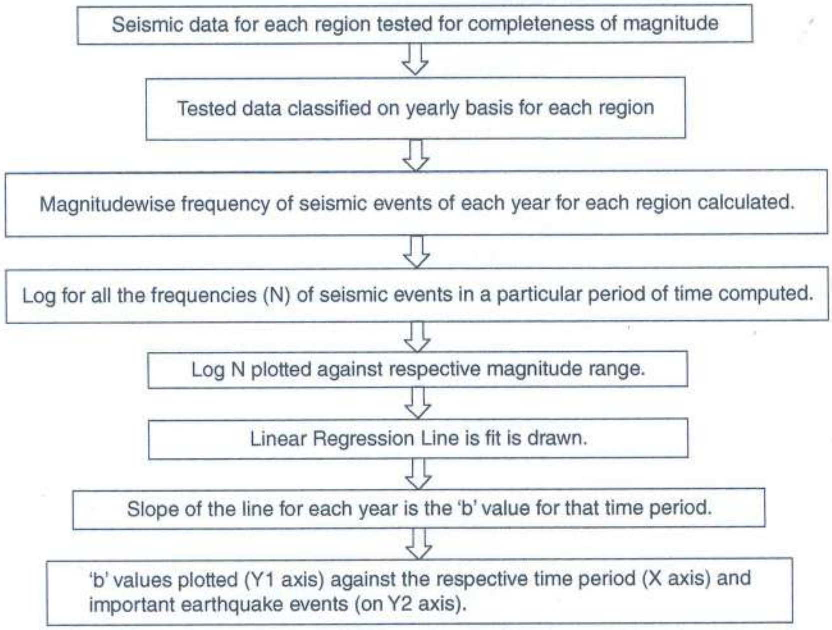

Figure 22.3 Methodology of computation of temporal "*b*" values in this work.

to correlate the same with major seismic events in the specific region. Accurate knowledge of magnitude of completeness (M_c) is essential for many seismicity-based studies, and particularly for mapping seismicity parameters (Woessner and Wiemer 2005). The M_c is defined as the lowest magnitude at which all the events in a space–time volume are detected (Rydelek and Sacks 1989; Taylor et al. 1990; Wiemer and Wyss 2000). After checking M_c, respective threshold magnitudes are decided and seismic data above a particular magnitude are analyzed.

At the same time, there should be a clear understanding of whether to include or exclude foreshocks and aftershocks into the *b*-value analyses. The number of aftershocks and the area affecting the aftershock are related to the main shock magnitude (review and original work by Christophersen and Smith 2000). The foreshocks and aftershocks of seismicity are clubbed together as the accessory shocks. No universally accepted physical basis exists at present to accurately separate the accessory shocks from the main shock (Musson 2000).

The "*b*" values are computed by the least squares method. The USGS earthquake catalog is used for this purpose. The earthquake records provide data of earthquake epicenters for location, date, magnitude, depth, region name, and others. The first three parameters are used to compute the "*b*" values. The catalog is found to be complete for seismicity with $M >$ 3.0. For some years, especially in the Chilean and Japanese regions (1986, 1989, 1991, 2009 for the Chilean region and 1991, 1998 Japanese region), the catalog is not complete and "*b*" values could not be computed. Such problems of incomplete catalog, in general, have also been pointed out by previous researchers (e.g. Zuniga and Wyss 1995).

22.2.6 Analyses and Results

The chosen four seismo-tectonically active regions recently experienced large earthquakes ($M > 8.0$). Seismic data for each region is analyzed independently for computation of "*b*" values and then correlated with major seismic events in the respective regions. The select extent of each region represents $10° \times 10°$ longitudinal and latitudinal areas around the recent major earthquakes.

1) Nepal Region: (Extent: 23 °N to 32 °N and 79 °E to 89 °E; location of the recent major earthquake: 28 °9′N × 84 °42′E)

   Nepal experienced 20 earthquakes of magnitude >6.00 from 1965 to 2015 (Figure 22.4). Earthquake records from 1976 to 2015 are considered for "*b*" value analysis considering the completeness of the earthquake catalog (USGS) for the region. The pattern of "*b*" values (Figure 22.5) shows that there are two conspicuous drops during 1986–1990 and 2011–2015. Both these drops are followed by the earthquakes of $M = 6.9$ in 1988 and $M = 7.8$ in 2015. Note that after the year 2000, the downward trend in "*b*" values is more prominent and there is no earthquake with $M \geq 7.0$. This indicates that crustal stresses accumulated, which were released in 2015 in the form of the Gorkha earthquake ($M = 7.8$).

2) Indonesian Region: (2 °S to 8 °N and 91 °E to 100 °E; location of the recent major earthquake: 3 °N × 96 °E).

   The Indonesian region has not experienced earthquakes of $M \geq 8.0$ from 1966 to 2004 (Figure 22.6). This clearly indicates the phase of accumulation of crustal stresses.

   An inverse relation between "*b*" value and seismic events is revealed for the Indonesian region as well (Figure 22.7). The region experienced an earthquake of $M = 7.7$ in

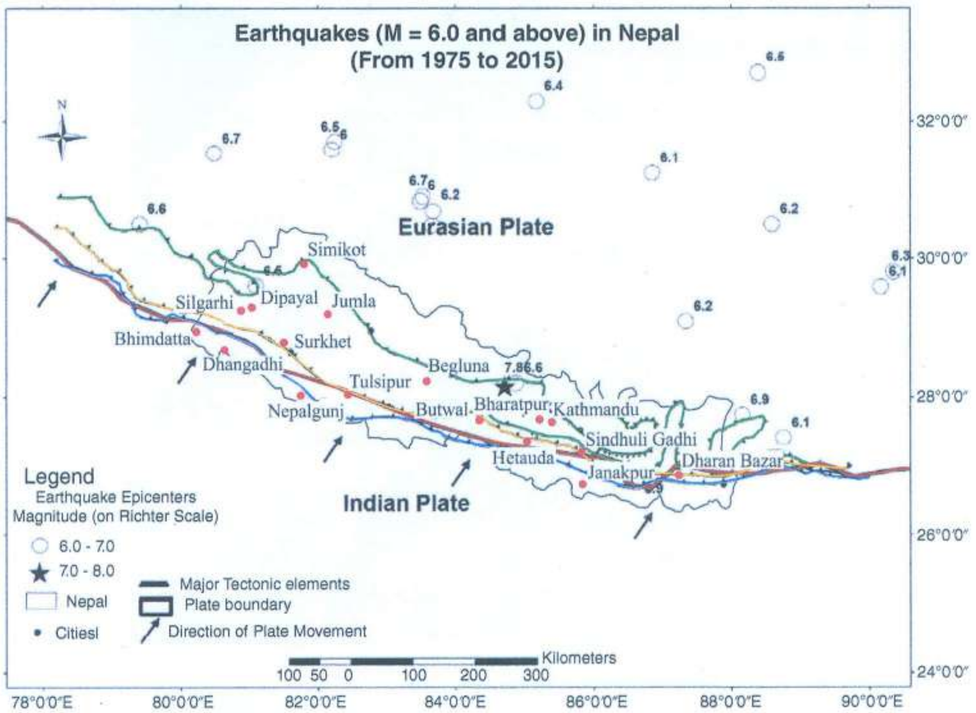

Figure 22.4 Major seismic events in Nepal from 1975 to 2005.

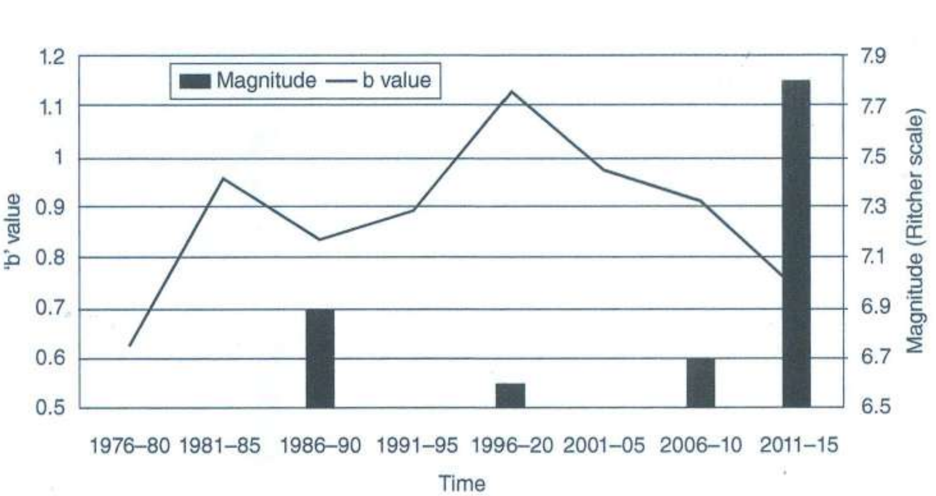

Figure 22.5 Temporal variations (1976 to 2015) in "*b*" values: Nepal Region. *Source:* Data source: USGS Earthquake catalog.

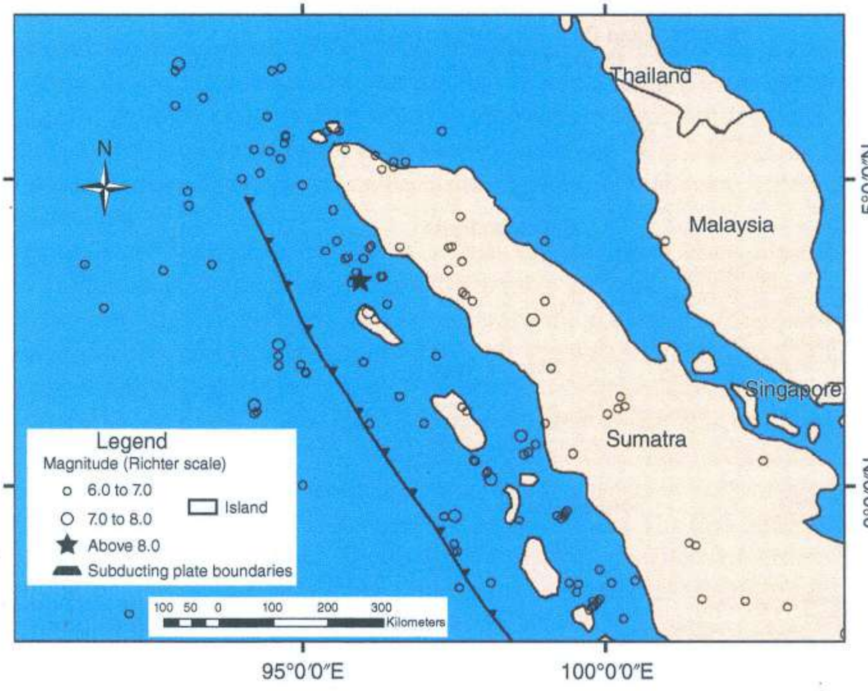

Figure 22.6 Major seismic events in the Indonesian region from 1966 to 2014.

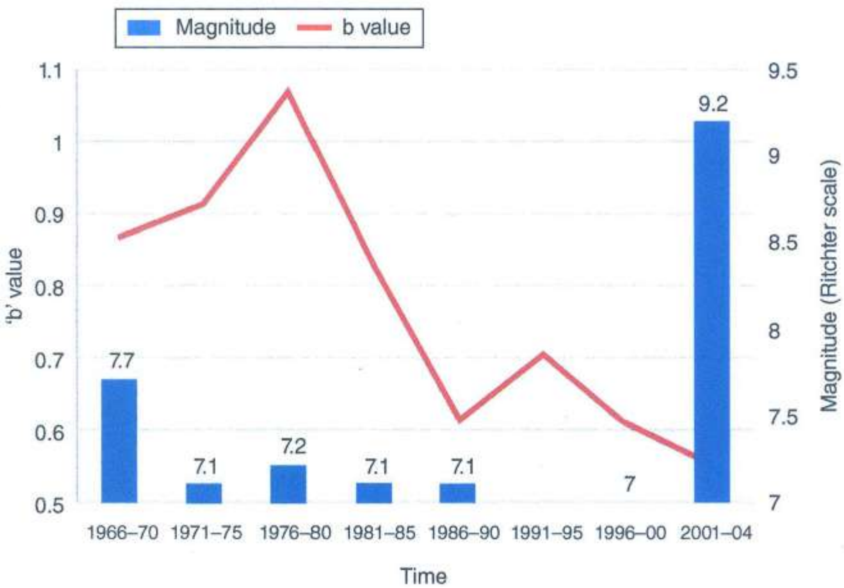

Figure 22.7 Temporal variations (1966–2004) in "*b*" values in the Indonesian region. *Source:* Data source: USGS Earthquake catalog.

1969. Thereafter, there has not been an earthquake of $M > 7.5$ till 2002, except for one event of $M = 7.6$. Since 1981, a falling trend of "b" value is observed, indicating that the region has been accumulating stress as the frequency of earthquakes is decreasing in the region. The lowest "b" value is observed during 2001–2005, the period in which the major earthquake ($M = 9.2$, dated 26 December 2004) struck.

3) Japanese Region: (extent: 131 °E to 144 °E longitude and 29 °N to 45 °N latitude, location of the recent major earthquake: 38.4 °N × 142.4 °E).

Figure 22.8 presents the earthquakes of $M > 7.0$ (from 1973 to 2013) in the Japanese region. The earthquakes are concentrated more in the region off the eastern coast of

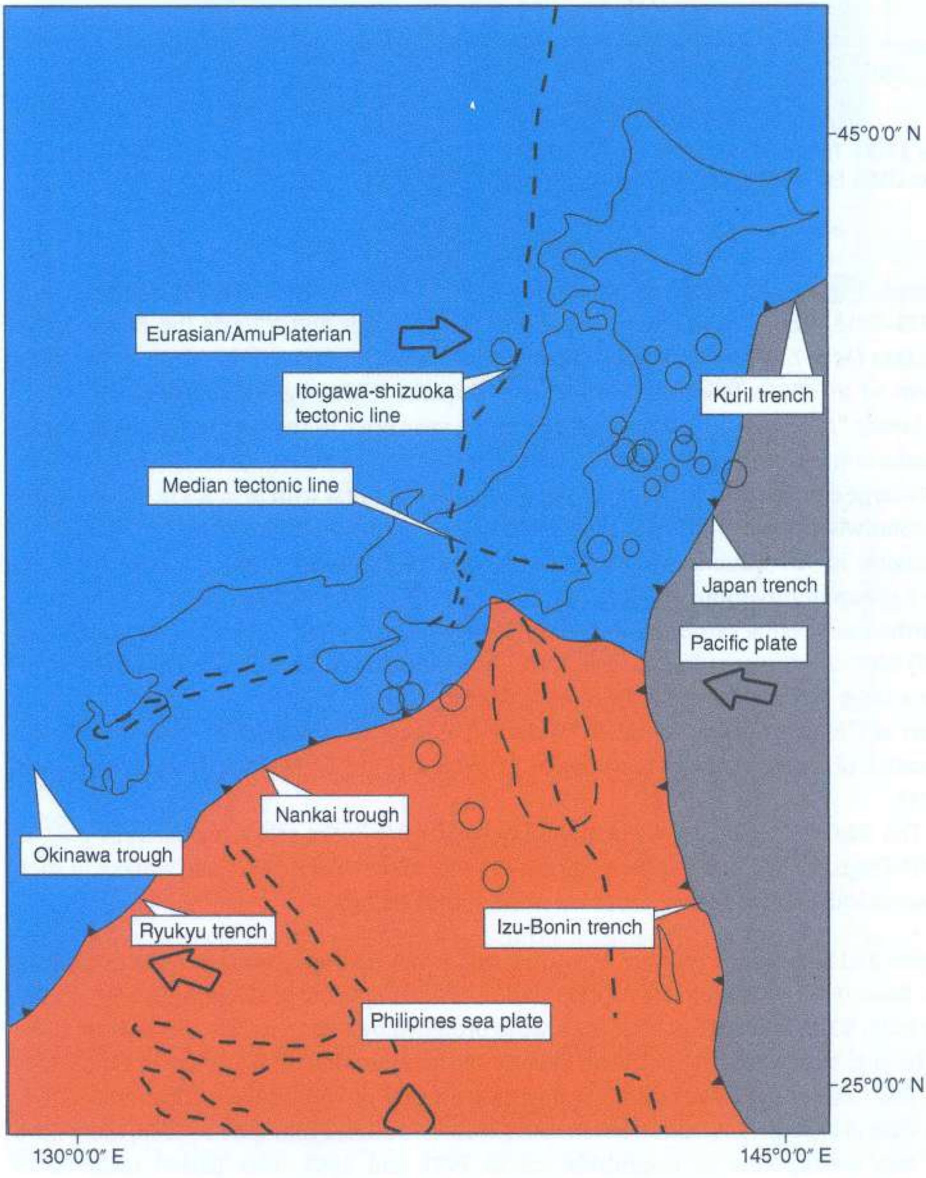

Figure 22.8 Major seismic events in the Japanese region from 1973 to 2013.

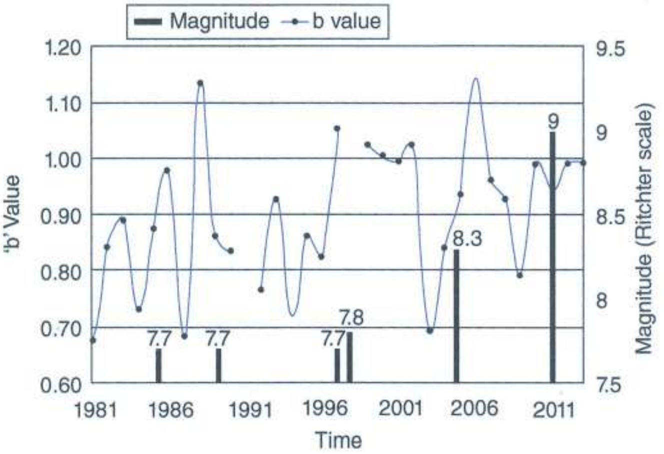

Figure 22.9 Temporal variations (1973–2013) in "b" values in the Japanese region. *Source:* Data source: USGS Earthquake catalog.

Japan. Figure 22.9 presents the trend of "b" values in the Japanese region during 1973–2013. The Y1-axis shows variations in "b" values and Y2-axis the major earthquakes ($M > 7.5$) The "b" values range from 0.6 to 1.1. It is noted that drop in "b" value from ~1 to <0.8 is followed by a major earthquake in the region (Figure 22.6).

Lower "b" values are observed either in the year prior to the year of the major earthquake or in the same year, wherein the major earthquake has occurred. There have been two large earthquakes in the region in this period: the first with $M = 8.3$ in 2003 and the second with $M = 9.0$ in 2011. Both earthquakes are preceded by lower "b" values. An increase in "b" value is also marked after the earthquakes of $M > 7.0$ have occurred in a group of three/four consecutive years identified. Some groups of years with major earthquake events can be prominently identified – (i) 1981–1984, (ii) 2003–2005, and (iii) 2008–2012, except for the year 2010 – no event of $M > 7.0$, seems to be compensated by a large earthquake of $M = 9.0$ on 11 March 2011.

4) Part of Chilean Coast (Extent: 65 °W to 76 °W longitudes and 25 °S to 36 °S latitudes; location of the recent major earthquake: 31°.57 S × 71°.65 W, M = 8.0, date: 16 September 2015.

   The Chilean region shows earthquakes of $M < 8.0$ in the select region from 1981 to 2016 (Figure 22.10). As in other regions, the very absence of a major earthquake in such a seismically active region connotes stress accumulation.

Figure 22.11 shows the trend of "b" values and major earthquakes in the part of Chilean coast. Since 1981, this area has experienced three earthquakes of magnitude >8.0, in the years 1985, 2010, and 2015, which are always preceded by a drop in "b" values. Note there have been gaps in acquiring sufficient data for the computation of "b" values in 1986, 1989, 1991, and 2009. Notwithstanding the downward trend of "b" values evident since 1996, there were also occasional mild rises in 2005, 2012, and 2015. From 1981 to 1985, there have been two earthquakes of magnitude 7.2 in 1981 and 1983. This period must be of

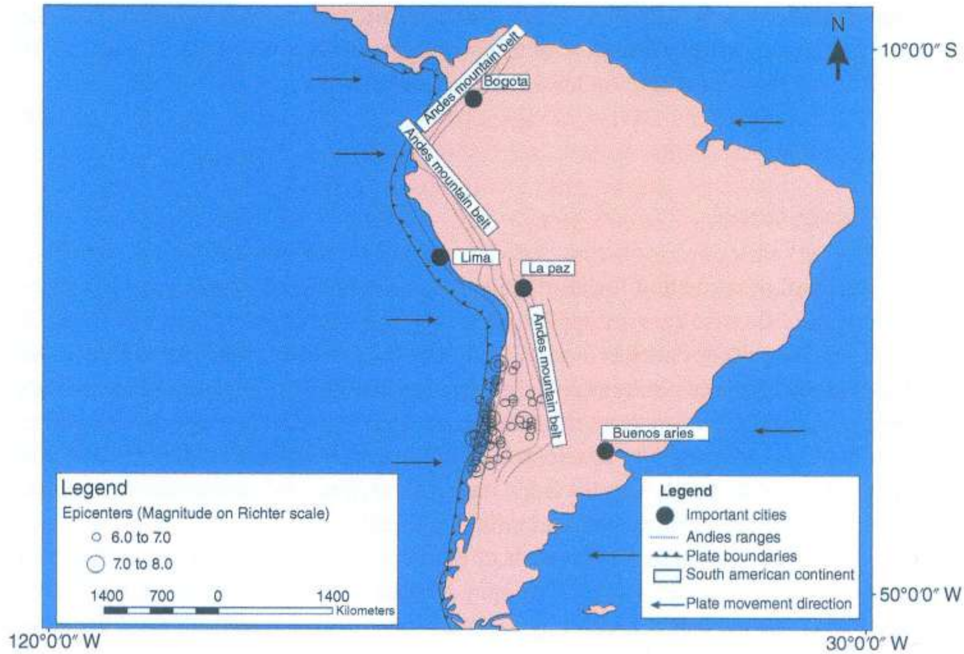

Figure 22.10 Major seismic events in the Chilean Region from 1981 to 2016.

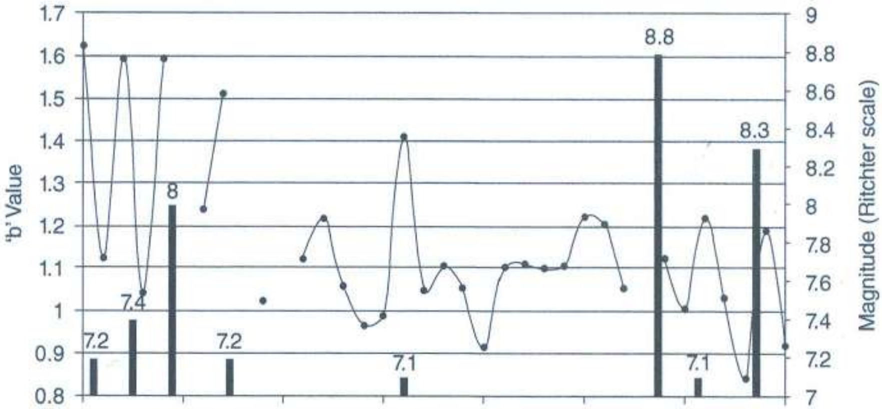

Figure 22.11 Temporal variations (1981 to May 2016) in "*b*" values: Chilean 772 region. *Source:* Data source: USGS Earthquake catalog.

accumulating stresses as there are only two of these events and that too $M < 7.5$. The major earthquake of 1985 – $M = 8.0$ (on 3 March 1985) can be seen as the result of accumulated stresses. It would have been far more interesting if the seismic records before the year 1981 were available. Since the 1985 event, there have been only two earthquakes of $M = 7.2$

(5 February 1988) and $M = 7.1$ (15 December 1997) till the next major earthquake ($M = 8.8$; 27 February 2010) occurred. Note that all the major events ($M = 8.0$, 1985; $M = 8.8$, 2010; and $M = 8.3$, 2015) are preceded by lower "*b*" values.

22.3 Discussions

The data gaps and the dearth of lower magnitude ($M < 3.0$) data are the main limitations. So, the rationale of this work can be applied effectively solely to higher magnitude ($M > 7.5$) events. If lower-magnitude data were available, the technique would apply for medium- and low-magnitude earthquake events as well. Due to the same limitation, it was not possible to compute the annual "*b*" values from the Indonesian and the Nepalese regions. The annual variations in "*b*" values might be able to predict seismicity. The time period for which the complete data is available also varies from region to region. The uniformity of the time period for data analysis could not be maintained perfectly.

In this work, only one section from each of the four seismically active zones has been considered to analyze the "*b*" values. One may also go for computing "*b*" values for the entire seismically active zones, section by section. This can give a better idea of the stress conditions in the regions and temporally rhythmic patterns in stress conditions if any. Along with the "*b*" value, other precursors such as seismic gap, V_p/V_s ratio, the electrical conductivity of groundwater, ground tilt, etc., demand attention as the future work.

Lowering of *b*-value connotes high-stress regime and vice versa. The fall of *b*-value indicates greater stress and subsequent seismicity (Andaman-Sumatra region: Nuannin 2006).

What we conclude from the chosen terrain may not hold true in other places. For example, Jafari (2008) compiled *b*-values from Iran but did not find any clear-cut relation between seismicity and *b*-value variations. Seo et al. (2010)-compiled *b*-values in the Korean peninsula do not show any conclusive pattern between *b*-values, which has an average magnitude of 0.96, and seismicity. Amorese et al. (2010) pointed out that depthwise *b*-value variation may not yield unequivocal conclusions. More specifically, the *b*-value can reduce linearly with depth in the continental crust, and can be dependent on the age of rocks in subduction zones (review in Scholz 2015; also see Enescu et al. 2011). Also, the *b*-value falls linearly as the differential stress increases, and vice versa (Scholz 2015).

Okal and Romanowicz (1994) reported an increase in *b*-value with seismicity size. A laboratory study revealed that the subduction zones are characterized by a linear relationship between the *b*-values and the slab pull force (Scholz 2015). A low *b*-value at ~30 km depth was linked with a specific ongoing tectonic deformation (Khan et al. 2011). Cao and Gao (2002) correlated the fall in *b*-value in the Japan island arc region from 0.86 during 1984–1990 to 0.73 during 1991–1995 to not just the seismicity but also the subduction rate.

Enescu et al. (2011) pointed out that *b*-value reduced before the 1995 Kobe seismicity (Japan). A similar report of *b*-value fall during a major quake has been made also from the Pollino range (southern Italy, Passarelli et al. 2015). Patwardhan (2012) reached the same conclusion in general from several terrains. However, recently, Nanjo and Yoshida (2017) pointed out an increase in *b*-value by an amount of 0.3–0.5 preceding the *M*7.3 earthquake in Kumamoto (16 April 2016; Japan). The *b*-value may decrease (Imoto 1991) or even increase before seismicity, and therefore cannot be used reliably in predicting seismicity (review in Burroughs and Tebbens 2002). Shi and Bolt (1982) through statistical analyses inferred that the *b*-value cannot be used to predict seismicity of magnitude >5 from central California. Henderson et al. (1994) deduced a negative correlation between *b*-value and fractal dimension of epicenter locations in Brazil. Yu (2016) recently referred that the "*b*-value ratio" would be a better predictor of seismicity than merely the *b*-value. Srivardhan and Srinu (2014) discussed the usefulness of predicting the aftershocks using the *b*-values. The *b*-values can fluctuate in a stressed region during crack propagation (Main et al. 1989).

The global average *b*-value is known to be ~1 (1.02 ± 0.03 to be more precise: El-Esa and Eaton 2014). The *b*-values < than the global average indicate the total energy released by earthquakes is < than the energy gathered. El-Esa and Eaton (2014) reviewed a global variation of *b*-value to be $0.3 \leq b \leq 2.5$. They concluded through their global review that *b*-value varies due to changes in effective stress. Less sampling, errors in magnitudes, and inhomogeneous capability for detection are the loopholes in predicting seismicity using *b*-values (review in Kamer 2014).

Even though the *b*-value has been researched for earthquake prediction (Manna et al. 2015), its physical significance has remained indeterminate (Cheng and Sun 2018).

22.4 Conclusions

In this article, the trend in "*b*" values and major seismic events are correlated with each other for sections of four seismically active zones in the world. After computing "*b*" values for >25 years of data for each of these regions, it is found that the range of "*b*" values varies from region to region, but a similar pattern in the case of a trend of "*b*" values and the major events is observed in all the four regions studied. The result can be terrain-specific since a different relationship has also been found in other places of the world.

In all the four chosen regions, the major seismic events are categorically preceded by lows in "*b*" values (Table 22.1). This in fact implies that the trend in "*b*" values in the respective region is more important than the absolute values of "*b*". Though the value of "*b*" per se cannot be correlated to a specific range of earthquake magnitude, the trend in "*b*" values

Table 22.1 The "*b*" value ranges, specific "*b*" values, and major events for the select regions.

Region	Highest "*b*" value	Lowest "*b*" value	Specific "*b*" value before the major event (year)	Magnitude of major earthquake on Richter scale (year)
Nepal	1.12	0.65	0.75 (2011–2015)	7.8 (2015)
Indonesia	1.05	0.55	0.55 (2001–2004)	9.2 (2004)
Japan	1.15	0.68	0.95 (2010)	9.0 (2011)
Chile coast	1.65	0.85	0.84 (2014)	8.3 (2015)

shows a correlation with the earthquake magnitude. The value of "*b*" itself is not indicative of the stress conditions and varies spatially and temporally, but the trend does indicate the stress conditions in the respective region and, thus, an impending earthquake.

It is also found that immediately before a major event, there is a slight increase in "*b*" values (Japan region – before the earthquake of 2005 [$M = 8.3$], the "*b*" value increased from 0.7 to 0.85 and in Chilean region from 0.85 to 9 before the earthquake of 2015 [$M = 8.3$]) in "*b*" value. This indicates increased frequency of small earthquakes in the region, just before the major event. Considering the results of the analysis, it is concluded that "*b*" value can be applied as an indicator that will give an idea about the relative stress conditions in a region. If "*b*" decreases in a region than the previous time periods, then it should be taken as an indication of an impending earthquake.

Reviewing the past trend of research, Sykes et al. (1999) expected that long-term (10–30 years) and intermediate-term (1 month to 10 years) seismicity might be possible to predict in tectonically very active areas. Interestingly, the study areas we have chosen in this article are tectonically active as per Sykes et al.'s (1999) requirement.

Acknowledgments

Late Dr. S. K. Guha (Central Water and Power Research Station, Khadakwasla, Pune) inspired Deepali Gadkari to undertake this work. His guidance and experience in the field of earthquake science made this work possible. Support by Prof. S. R. Jog (Department of Geography, S. P. University of Pune) is also thanked. The administrative help and support extended by the Head, Department of Geography, University of Mumbai, Mumbai is acknowledged. Merryl Le Roux, Frank Otmar Weinreich, Joss Everett, Andrew Harrison, and the proofreading team (Wiley Blackwell) are thanked for their assistance. CPDA grant (IIT Bombay) supported SM. This chapter has been encapsulated in Mukherjee et al. (2023).

References

Amorese, D., Grasso, J.-R., and Rydelek, P.A. (2010). On varying b-values with depth: results from computer-intensive tests for southern California. *Geophys J Int* 180: 347–360.

Ayyub, B.M. and RH, M.C. (2011). *Probablility, Statistics, and Reliability for Engineers and Scientists*, 3e, 105. Boca Raton, FL: CRC Press. ISBN: ISBN −13: 978-1-4398-9533-7.

Bangs, N.L.B., Gulick, S.P.S., and Shipley, T.H. (2006). Seamount subduction erosion in the Nankai trough and its potential impact on the seismogenic zone. *Geology* 34: 701–704.

Barrientos, S., Vera, E., Alvarado, P., and Monfret, T. (2004). Crustal seismicity in Central Chile. *J South Am Earth Sciences* 16: 759–768.

Bohm, M., Luth, S., Echtler, H. et al. (2002). The southern Andes between 36° and 40°S latitude: seismicity and average seismic velocities. *Tectonophysics* 356: 275–289.

Bollinger, L., Perrier, F., Avouac, J.-P. et al. (2007). Seasonal modulation of seismicity in the Himalaya of Nepal. *Geophys Res Lett* 34: L08304.

Burroughs, S.M. and Tebbens, S.F. (2002). The upper-truncated power law applied to earthquake cumulative frequency–magnitude distributions: evidence for a time-independent scaling parameter. *Bull. Seismol. Soc. Am.* 92: 2983–2993.

Cao, A. and Gao, S.G. (2002). Temporal variation of seismic *b*-values beneath northeastern Japan island arc. *Geophys Res Lett* 29: https://doi.org/10.1029/2001GL013775.

Cheng, Q. and Sun, H. (2018). Variation of singularity of earthquake-size distribution with respect to tectonic regime. *Geosci. Front.* 9: 453–458.

Christophersen A, Smith GC. 2000. A global model for aftershock behavior. *12WCEE conference* 0379.

Daly, M.C., Cooper, M.A., Wilson, I. et al. (1991). Cenozoic plate tectonics and basin evolution in Indonesia. *Mar. Pet. Geol* 8: 2–21.

Das, S. (2004). Seismicity gaps and the shape of the seismic zone in the Banda Sea region from relocated hypocenters. *J Geophys Res* 109: B 1203.

DeCelles, P., Robinson, D.M., Quade, J. et al. (2001). Stratigraphy, structure, and tectonic evolution of the Himalayan fold-thrust belt in western Nepal. *Tectonics* 20: 487–509.

Delouis, B., Cisternas, A., Dorbath, L. et al. (1996). The Andean subduction zone between 22 and 25°S (northern Chile): precise geometry and state of stress. *Tectonophysics* 259: 81–100.

El-Esa, Z.H. and Eaton, D.W. (2014). Spatiotemporal variations in the b-value of earthquake magnitude–frequency distributions: classification and causes. *Tectonophysics* 615-616: 1–11.

El-Nader, I.F.A., Shater, A., and Hussein, H.M. (2016). Mapping b-values beneath Abu Dabbab from June to august 2004 earthquake swarm. *NRIAG J.Astron.Geophys* 5: 403–412.

Enescu, B., Enescu, D., and Eto, K. (2011). Values of b and p: their variations and relation to physical processes for earthquakes in Japan and Romania. *Rom.J.Phys* 56: 590–608.

Engdahl, E.R., Villasenor, A., DeShon, H.R., and Thurber, C.H. (2007). Teleseismic relocation and assessment of seismicity (1918–2005) in the region of the 2004 *M*w 9.0 Sumatra–Andaman and 2005 *M*w 8.6 Nias Island great earthquakes. *Bull. Seismol. Soc. Am* 97: S43–S61.

Farias, M., Comte, D., Charrier, R. et al. (2010). Crustal-scale structural architecture in central Chile based on seismicity and surface geology: implications for Andean mountain building. *Tectonics* 29: TC3006.

Fiedler, G.B. (1974). Local b-values related to seismicity. *Tectonophysics* 23 (3): 277–282.

Gerbault, M., Cembrano, J., Mpodozis, C. et al. (2009). Continental margin deformation along the Andean subduction zone: thermo-mechanical models. *Phys. Earth Planet. Inter* 177: 180–205.

Gibowicz, S.J. (1973). Variation of the frequency-magnitude relation during earthquake sequences in New Zeland. *Bull. Seism. Soc. Am.* 63: 517–528.

Guha, S.K. (1983). Seismo-statistical modelling of tectonic stress-building process. In: *Proc, Workshop on Geomodelling* (ed. B.K. Sahu), 138–143. Bombay: IIT.

Gutenberg, B. and Richter, C.F. (1944). Frequency of earthquakes in California. *Bull. Seism. Soc. Am* 34: 185–188.

Henderson, J., Main, I.G., Pearce, R.G., and Takeya, M. (1994). Seismicity in North-Eastern Brazil: fractal clustering and the evolution of the *b* value. *Geophys. J. Int* 116: 217–226.

Huang, J. and Turcotte, D.L. (1988). Fractal distributions of stress and strength and variations of b-value. *Earth Planet. Sci. Lett* 91: 223–230.

Imoto, M. (1991). Changes in the magnitude-frequency b-value prior to large (M > 6.0) earthquakes in Japan. *Tectonophysics* 193: 311–325.

Isozaki, Y., Aoki, K., Nakama, T., and Yanai, S. (2010). New insight into a subduction-related orogen: a reappraisal of the geotectonic framework and evolution of the Japanese Islands. *Gondwana Research* 18: 82–105.

Iyer, H.M. (1976). Earthquake prediction – present status. In: *Earthquake Prediction: How Close Is it to Reality* (ed. S.K. Guha and A.M. Patwardhan), 1–11. Pune, India: University of Poona.

Jafari, M.A. 2008. The distribution of b-values in different seismic provinces of Iran. *The 14th World Conference on Earthquake Engineering*. (12–17 October). Beijing. China.

Kamer, Y. (2014). Minimum sample size for detection of Gutenberg-Richter's b-value. *arXiv* 1410.1815v1.

Khan, P.K., Ghosh, M., Chakraborty, P.P., and Mukherjee, D. (2011). Seismic *b*-value and the assessment of ambient stress in Northeast India. *Pure Appl. Geophys* 168: 1693–1706.

Klotz, J., Khazaradze, G., Angermann, D. et al. (2001). Earthquake cycle dominates contemporary crustal deformation in central and southern Andes. *Earth Planet. Sci. Lett* 193: 437–446.

Kodaira, S., Kurashimo, E., Park, J.-O. et al. (2002). Structural factors controlling the rupture process of a megathrust earthquake at the Nankai trough seismogenic zone. *Geophys J Int* 149: 815–835.

Lallemand, S. and Le Pichon, X. (1987). Coulomb wedge model applied to the subduction of seamounts in the Japan trench. *Geology* 15: 1065–1069.

Landgraf, A., Kübler, S., Hintersberger, E. & Stein, S. 2017. Active tectonics, earthquakes and palaeoseismicity in slowly deforming continents. In: Landgraf, A., Kübler, S., Hintersberger, E. & Stein, S. (Eds) *2017. Seismicity, Fault Rupture and Earthquake Hazards in Slowly Deforming Regions*. Geological Society, London, Special Publications, 432, 1–12.

Lange, D., Rietbrock, A., Haberland, C. et al. (2007). Seismicity and geometry of the south Chilean subduction zone (41.5°S-43.5°S): implication for controlling parameters. *Geophys Res Lett* 34: L06311.

Lange, D., Tilmann, F., Rietbrock, A. et al. (2010). The fine structure of the subducted investigator fracture zone in Western Sumatra as seen by local seismicity. *Earth Planet. Sci. Lett* 298: 47–56.

Lasitha, S., Radhakrishna, M., and Sanu, T.D. (2006). Seismically active deformation in the Sumatra-Java trench-arc region: geodynamic implications. *Curr. Sci* 90: 690–696.

Liu, Y. and Zhu, S.B. (2010). Comparison of the 1999Chi-Chi Mw7.6 earthquake and the 2008 Wenchuan MS 8.0 earthquake. In: *Rock Stress and Earthquakes* (ed. F. Xie), 659–664. London: Taylor & Francis Group.

Main, I.G., Meredith, P.G., and Jones, C. (1989). A reinterpretation of the precursory seismic b-value anomaly from fracture mechanics. *Geophys. J* 96: 131–138.

Malgrange, M., Deschamps, A., and Madariaga, R. (1981). Thrust and extensional faulting under the Chilean coast: 1965, 1971 Aconcagua earthquakes. *Geophys J Int* 66: 313–331.

Manna, S., Paul, H., and Mitra, S. (2015). B-value characterization of earthquakes in the eastern Himalayan and indo-Burman plate boundary system. *AGU Abstract.*.

McCaffrey, R. (1989). Seismological constraints and speculations on Bandra arc tectonics. *Neth.J. Sea Res* 24: 141–152.

McCaffrey, R. (2009). The tectonic framework of the Sumatran subduction zone. *Annu. Rev. Earth Planet. Sci* 37: 345–366.

McCann, W. R., Nishenko, S. P., Sykes, L. R. Krause, J. (1978) Seismic gaps and plate tectonics: seismic potential for major plate boundaries in proceedings of conference VI – methodology for identifying seismic gaps and soon – to – break gaps. U.S. Geological Survey Open-File Report 78-943: 441–584.

Metcalfe, I. (2011). Tectonic framework and Phanerozoic evolution of Sundaland. *Gondwana Research* 19: 3–21.

Miura, S., Kodaira, S., Nakanishi, A. et al. (2003). Structural characteristics controlling the seismicity of southern Japan trench fore-arc region, revealed by ocean bottom seismographic data. *Tectonophysics* 363: 79–102.

Mogi, K. (1990). Seismicity before and after large shallow earthquakes around the Japanese islands. *Tectonophysics* 175: 1–33.

Mueller C.S, Frankel A.D, Petersen M.D, Leyendecker, E.V. 1997. Documentation for 2003 USGS seismic Hazard maps for Puerto Rico and the U.S. Virgin Islands, open-file report 03-379, U.S. Geological Survey.

Mukherjee, S. (2015). A review on out-of-sequence deformation in the Himalaya. In: *Tectonics of the Himalaya*, vol. 412 (ed. S. Mukherjee, R. Carosi, P. van der Beek, et al.), 67–109. Geological Society, London. Special Publications.

Mukherjee, S., Dasgupta, S., Majumdar, C. et al. (2023). Introduction to: Handbook of Petroleum Geoscience: Exploration, Characterization, and Exploitation of Hydrocarbon Reservoirs. In: *Handbook of Petroleum Geoscience: Exploration, Characterization, and Exploitation of Hydrocarbon Reservoirs*, Petroleum Industry Updates: Geoscientific and Economic Issues (ed. S. Mukherjee, S. Dasgupta, C. Majumdar, et al.). John Wiley & Sons, Hoboken, ISBN 978-1-119-68003-1.

Musson, R.M.W. (2000). Generalized seismic hazard maps for the Pannonian basin using probabilistic methods. *Pure Appl. Geophys* 157: 147–169.

Nanjo, K.Z. and Yoshida, A. (2017). Anomalous decrease in relatively large shocks and increase in the *p* and *b* values preceding the April 16, 2016, *M*7.3 earthquake in Kumamoto, Japan. *Earth, Planets and Space* 69: 13.

Nuannin P. 2006. The Potential of *b*-value variations as earthquake precursors for small and large events. Ph.D. thesis. Uppsala University.

Nuannin, P., Kulhanek, O., and Persson, L. (2005a). Spatial and temporal b value anomalies preceding the devastating off coast of NW Sumatra earthquake of December 26, 2004. *Geophys. Res. Lett* 32: L11307.

Nuannin, P., Kulhanek, O., Persson, L., and Askemur, T. (2005b). Inverse correlation between induced seismicity and b-value, observed in the Zingruvan mine. *Sweden. Acta Geodyn. Geomater* 2: 5–13.

Nuannin, P., Kulhanek, O., and Persson, L. (2012). Variations of b-values preceding large earthquakes in the Andaman–Sumatra subduction zone. *J. Asian Earth Sci* 61: 237–242.

Okal, E.A. and Romanowicz, B.A. (1994). On the variation of b-values with earthquake size. *Phys. Earth Planet. Inter* 87: 55–76.

Pandey, M.R., Tandukar, R.P., Avouac, J.P. et al. (1995). Interseismic strain accumulation on the Himalayan crustal ramp (Nepal). *Geophys Res Lett* 22: 751–754.

Pandey, M.R., Tandukar, R.P., Avouac, J.P. et al. (1999). Seismotectonics of the Nepal Himalaya from a local seismic network. *J Asian Earth Sci* 17: 703–712.

Passarelli, L., Hainzl, S., Cesca, S. et al. (2015). Aseismic transient driving the swarm-like seismic sequence in the Pollino range, southern Italy. *Geophys. J. Int* 201: 1553–1567.

Patil, N., Guha, S.K., and Powar, K.B. (1986). Seismic risk evaluation of Northeast India. In: *Earthquake Prediction: Present Status* (ed. S.K. Guha and A.M. Patwardhan), 235–246. Pune, India: University of Poona.

Patwardhan, A.M. (2012). *The Dynamic Earth System*, 3e, 484. New Delhi: PHI Learning Private Ltd.

Perucca, L. and Bastias, H. (2008). Neotectonics, seismology and paleoseismology. In: *The Late Cenozoic Pantagonia and Tierra Del Fuego. Developments in Quaternary Sciences 11* (ed. J. Rabassa), 73–94. Amsterdam: Elsevier. ISBN: 978-0-444-52954-1.

Petersen M.D, Frankel A.D, Harmsen S.C, Mueller C.S, Haller K.M, Wheeler R. L, Wesson R.L, Zeng Y, Boyd O S, Perkins D. M, Luco N, Field E.H, Wills C. J, and Rukstales K.S. 2008. Documentation for the 2008 update of the United States National Seismic Hazard Maps, open file report – 2008-1128; U.S. Department of the Interior U.S. Geological Survey.

Prawirodirdjo, L., Bock, Y., Genrich, J.F. et al. (2000). One century of tectonic deformation along the Sumatran fault from triangulation and Global Positioning System surveys. *J Geophys Res* 105: 28343–28361.

Rajendran, K., Parameshwaran, R.M., and Rajendran, C.P. (2017). Seismotectonic perspectives on the Himalayan arc and contiguous areas: inferences from past and recent earthquakes. *Earth Sci Rev* 173: 1–30.

Rydelek, P.A. and Sacks, I.S. (1989). Testing the completeness of earthquake catalogues and the hypothesis of self-similarity. *Nature* 337: 251–253.

Schelling, D. and Arita, K. (1991). Thrust tectonics, crustal shortening, and the structure of the far-eastern Nepal Himalaya. *Tectonics* 10: 851–862.

Scholz, C.H. (2015). On the stress dependence on the earthquake b value. *Geophys.Res.Lett* 42: 1399–1402.

Seo, J.M., Rhee, H.M., and Choi, I.K. (2010). A study on the best estimate of seismicity parameter b-value and its application for the seismic Hazard analysis of the Korean peninsula. *J.Earthq. Eng.Soc.Korea* 35: 42. https://doi.org/10.5000/EESK.2010.14.1.035.

Shi, Y. and Bolt, B.A. (1982). The standard error of the magnitude-frequency b-value. *Bull. Seismol. Soc. Am* 72: 1677–1687.

Shikazono, N. (2012). *Introduction to Earth and Planetary System Science: New View of Earth Planets and Humans. Springer*, 71. ISBN: 978-4-431-54058-8.

Singh HN, Paudyal H, Shanker D, Panthi A, Kumar A, Sinh VP. 2010. Anomalous seismicity and earthquake forecast in western Nepal Himalaya and its adjoining Indian region. *Pure Appl. Geophys*. DOI: https://doi.org/10.1007/s00024-010-0072-6

Smith, W.D. (1981). The b-value as an earthquake precursor. *Nature* 289: 136–139.

Sobiesiak, M., Meyer, U., Schmidt, S. et al. (2007). Asperity generating upper crustal sources revealed by b value and isostatic residual anomaly grids in the area of Antofagasta, Chile. *J. Geophys. Res.* 112: B12.

Srivardhan V, Srinu U. 2014. Potential of fractal analysis of earthquakes through wavelet analysis and determination of b value as an aftershock precursor: a case study using earthquake data between 2003 and 2011 in Turkey. *J. Earthq.*2014, article id 123092.

Stauder, W. (1973). Mechanism and spatial distribution of Chilean earthquakes with relation to subduction of the oceanic plate. *J Geophys Res* 78: 5033–5062.

Suarez, G., Molnar, P., and Burchfiel, B.C. (1983). Seismicity, fault plane solutions, depth of faulting, and active tectonics of the Andes of Peru, Ecuador, and southern Columbia. *J Geophys Res* 88: 10403–10428.

Sukmono, S., Zen, M.T., Hendrajaya, L. et al. (1997). Fractal pattern of the Sumatra fault seismicity and its possible application to earthquake prediction. *Bull. Seismol. Soc. Am.* 87: 1685–1690.

Sykes, L.R., Shaw, B.E., and Scholz, C.H. (1999). Rethinking earthquake prediction. *Pure and Applied Geophysics* 155: 207–232.

Tanioka, Y., Ruff, L., and Satake, K. (1997). What controls the lateral variation of large earthquake occurrence along the Japan trench? *Island Arcs* 6: 261–266.

Tassara, A. and Echaurren, A. (2012). Anatomy of the Andean subduction zone: three-dimensional density model upgraded and compared against global-scale models. *Geophys. J. Int.* 189: 161–168.

Taylor, D.W.A., Snoke, J.A., Sacks, I.S., and Takanami, T. (1990). Non-linear frequency-magnitude relationship for the Hokkaido corner, Japan. *Bull. Seism. Soc. Am.* 80: 340–353.

The ANNCORP Working Group (1999). Seismic refection image revealing offset of Andean subduction-zone earthquake locations into oceanic mantle. *Nature* 397: 341–344.

Tsuru, T., Park, J.-O., Miura, S. et al. (2002). Along-arc structural variation of the plate boundary at the Japan trench margin: implication of interplate coupling. *J Geophys Res* 107: 2357.

U.S. National Academy of Sciences (1976). *Predicting Earthquakes – a Scientific and Technical Evaluation with Implications for Society*, 62. Washington, D.C.: Natnl. Acdm. of Scis.

Upreti, B.N. (1999). An overview of the stratigraphy and tectonics of the Nepal Himalaya. *J Asian Earth Sci* 17: 577–606.

Utsu, T. (1965). A method for determining the value of b in the formula log n = a-bM showing the magnitude frequency relation for earthquakes. Geophys. Bull. *Hokaido Univ.* 13: 99–103.

Wiemer, S. and Wyss, M. (2000). Minimum magnitude of complete reporting in earthquake catalogs: examples from Alaska, the Western United States, and Japan. *Bull. Seism. Soc. Am* 90: 859–869.

Woessner, J. and Wiemer, S. (2005). Assessing the quality of earthquake catalogues: estimating the magnitude of completeness and its uncertainty. *Bull. Seism. Soc. Am* 95: 684–698.

Wyss, M. (2014). *Earthquake Hazards, Risks and Disasters. Hazards and Disaster Series*, 123–124. Amsterdam: Elsevier. ISBN: 978-0-12-394848-9.

Xu, J. and Kono, Y. (2002). Geometry of slab, intraslab stress field and its tectonic implication in the Nankai trough, Japan. *Earth Planets Space* 54: 733–742.

Yu, D. (2016). Investigations of the b-value and its variations on possible earthquake prediction in the North-South China Seismic Belt. Doctoral Dissertation, Massachusetts Institute of Technology.

Zalohar, J. (2018). *The Omega-Theory: A New Physics of Earthquakes*, Developments in Structural Geology & Tectonics. Series Editor: S. Mukherjee, 131. Amsterdam: Elsevier. ISBN: 978-0-12-814580-7.

Zuniga, F.R. and Wiemer, S. (1999). Seismicity patterns: are they always related to natural causes? Pure Appl. *Geophys.* 155: 713–726.

Zuniga, F.R. and Wyss, M. (1995). Inadvertent changes in magnitude reported in earthquake catalogs: their evaluation through b-value estimates. *Bull SeismolSoc Am* 85: 1858–1866.

Web References

1. http://plcmets.pbworks.com/f/Tectonics+rate+map.jpg
2. http://montessorimuddle.org/2011/03/11/plate-tectonics-and-the-earthquake-in-japan